Hybrid Organic-Inorganic Halide Perovskites: Dimensionality vs. Applicability. A Theoretical Standpoint

Giacomo Giorgi

DIPARTIMENTO DI INGEGNERIA CIVILE ED AMBIENTALE
DICA

UNIVERSITÀ DEGLI STUDI DI PERUGIA

Perovskite, ABX_3 ($CaTiO_3$)

Gustav Rose, 1839

"A" & "B" ions are both cations with noticeable different radii."X" is an anion site.
Their stability is determined by the Goldschmidt tolerance factor "t" which in the case of X being an oxygen anion is given by

$$t = (R_A + R_O)/\sqrt{2}(R_B + R_O)$$

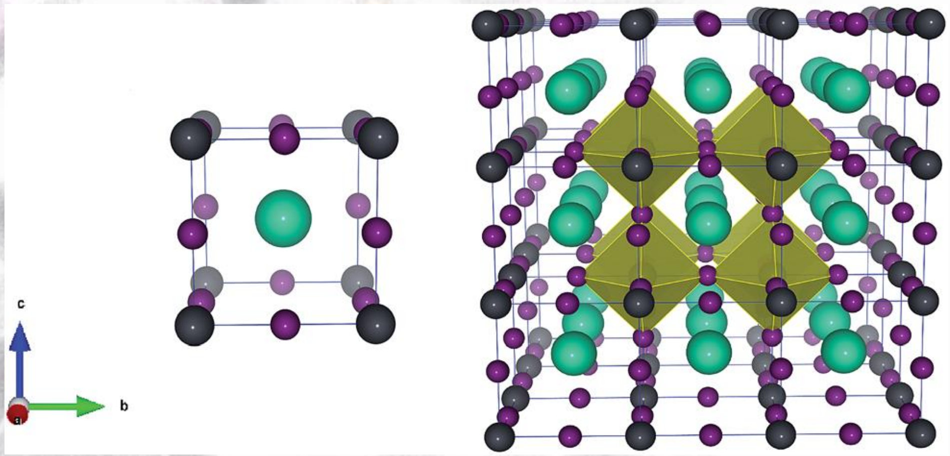

Piezoelectricity, pyroelectricity, colossal magnetoresistivity, high-T superconductivity, & electrooptic effects and many others… .

Although the oxide class represents the most abundant and investigated class of perovskites, halides, sulfides, nitrides, hydrides, oxyhalides, and oxynitrides are similarly known experimentally and have been characterized.

$CH_3NH_3PbX_3$, ein Pb(II)-System mit kubischer Perowskitstruktur

$CH_3NH_3PbX_3$, a Pb(II)-System with Cubic Perovskite Structure

Dieter Weber
Institut für Anorganische Chemie der Universität Stuttgart

Z. Naturforsch. **33 b,** 1443–1445 (1978); eingegangen am 21. August 1978

Synthesis, X-ray

$CH_3NH_3PbX_3$ (X = Cl, Br, I) has the cubic perovskite structure with the unit cell parameters a = 5,68 Å (X = Cl), a = 5,92 Å (X = Br) and a = 6,27 Å (X = I). With exception of $CH_3NH_3PbCl_3$ the compounds show intense colour, but there is no significant conductivity under normal conditions. The properties of the system are explained by a "p-resonance-bonding". The synthesis is described.

Im System $APbX_3$ (A = einwertiges Kation, X = Cl, Br, I) ist die Perowskitstruktur bislang nur bei Hochtemperaturmodifikationen des Typs $CsPbX_3$ [1, 2] bekannt. Dagegen kristallisiert das Sn(II)-analoge $CsSnBr_3$ [3–5] schon bei Normalbedingungen im kubischen Perowskitgitter. Vermutlich reicht die Größe des Cs^+-Kations nicht aus, um in einer Pb(II)-Perowskitstruktur den ihm zur Verfügung stehenden Raum so auszufüllen, daß die Kristallfeldenergie bei Raumtemperatur das Pb(II) in die Oktaedersymmetrie zwingt. Dementsprechend nimmt die Umwandlungstemperatur von

die kubischen Kristalle der Zusammensetzung $CH_3NH_3PbI_3$ schwarz sind. Die gemischthalogenierten Verbindungen lassen charakteristische Farbzwischenstufen erkennen. So verursacht die partielle Substitution von Bromid gegen Chlorid eine Farbaufhellung, wie die dunkelgelbe Farbe von $CH_3NH_3PbBr_{2,3}Cl_{0,7}$ verdeutlicht. Wird dagegen Bromid durch Iodid ersetzt wie im Fall von $CH_3NH_3PbBr_{2,3}I_{0,93}$, so macht sich dies in einer Farbvertiefung nach rotviolett bemerkbar. Das schwarze $CH_3NH_3PbBr_{0,45}I_{2,55}$ unterscheidet sich in der Farbe nicht mehr von $CH_3NH_3PbI_3$.

What are the organic-inorganic perovskites?

1) 2D crystal hybrid organic/inorganic: potential applications in optoelectronic due to the versatility of the organic part (Mitzi *et al.*, Science 1995)

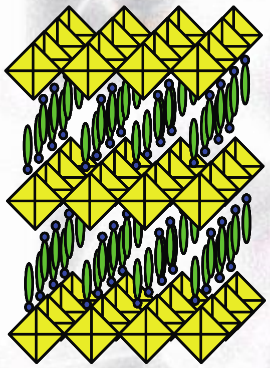

2) More recently, mixed organic-inorganic perovskite compounds as light harvester (Miyasaka *et al.*, JACS 2009 PCE=3.8%)

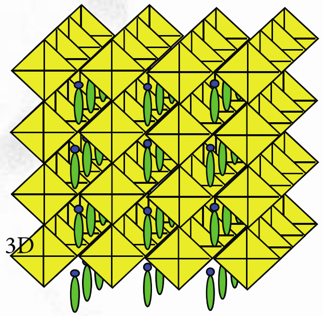

- Why are OIHPs so appealing for PV applications?

-How to use them in PV?

-Any possible improvement in their performances?

Perovskite compounds as light harvester (Miyasaka *et al.*, JACS 2009 PCE=3.8%)

- **Snaith *et al.*** (Science 2012)

"**MSSC**" (Mesosuperstructured solar cells) initially based on ETA concept

Perovskite absorber/mp-TiO_2(*n*-type)/spiro-OMeTAD (*p*-type)

- $CH_3NH_3PbI_2Cl$

- Insulating Al_2O_3 improves the PCE over mp-TiO_2 (PCE=10.9% @ AM1.5)

- **Grätzel *et al.***(Nature Phot.,2013)

(FTO)/TiO_2/perovskite/HTM/Au

- $CH_3NH_3PbI_3$ has ambipolar character

(*n*-type, *p*-type conductor)

-**HTM**: P3HT, PCPDTBT, PCDTBT, PTAA

-Using PTAA leads to PCE=12.0 % (standard AM 1.5)

Perovskite solar efficiency: 22.1% (WR)
2017 July
Ulsan National Institute of Science & Technology (UNIST).

Sept 2013, *Science*: **Snaith et al.**
(thin film, low T)
-Vapor-deposited: J_{sc}=21.5 mAcm^{-2}, V_{OC}=1.07 V *ff*=0.68, **PCE=15.4%**

-Solution-processed: J_{sc}=17.6 mAcm^{-2}, V_{OC}=0.84 V, *ff*=0.58, **PCE=8.6%**

→NANOSTRUCTURING PROCESS IS NOT MANDATORY

Polymorphism of $MAPbX_3$

TABLE I. Temperature dependent structural data of $CH_3NH_3^+ PbX_3^-$ (X = Cl, Br, I).

Phase	Temperature (K)	Crystal system	Space group	Lattice (pm)	Volume (10^6 pm^3)
$CH_3NH_3^+ PbCl_3^-$					
α	> 178.8	cubic	$P\,m3m$	$a =$ 567.5	182.8
β	172.9–178.8	tetragonal	$P\,4/mmm$	$a =$ 565.6 $c =$ 563.0	180.1
γ	< 172.9	orthorhombic	$P\,222_1$	$a =$ 567.3 $b =$ 562.8 $c =$ 1118.2	357.0
$CH_3NH_3^+ PbBr_3^-$					
α	> 236.9	cubic	$P\,m3m$	$a =$ 590.1(1)	206.3 (260 K)
β	155.1–236.9	tetragonal	$I\,4/mcm$	$a =$ 832.2(2) $c =$ 1183.2(7)	819.4
γ	149.5–155.1	tetragonal	$P\,4/mmm$	$a =$ 589.4(2) $c =$ 586.1(2)	
δ	< 144.5	orthorhombic	$P\,na2_1$	$a =$ 797.9(1) $b =$ 858.0(2) $c =$ 1184.9(2)	811.1
$CH_3NH_3^+ PbI_3^-$					
α	> 327.4	cubic	$P\,m3m$	$a =$ 632.85(4)	253.5
β	162.2–327.4	tetragonal	$I\,4/mcm$	$a =$ 885.5(6) $c =$ 1265.9(8)	992.6
γ	< 162.2	orthorhombic	$P\,na2_1$	$a =$ 886.1(2) $b =$ 858.1(2) $c =$ 1262.0(3)	959.5

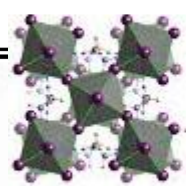

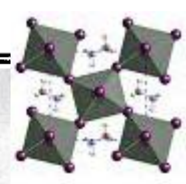

- 3D bulk analysis
  - The role of the organic cation:
    - Ambipolar nature of the OIHPs.
    - Alternative, bulky, and less polarizable organic cation (FAPI/GAPI).
    - Aliovalent substitution of Pb metallic cation.
  - Slow hot-hole cooling in lead-iodide perovskite: carrier lifetime from electron–phonon interaction.
  - The effects of the organic–inorganic interactions on the thermal transport properties of MAPI.

- 0D clusters:
  - Cluster applicability in photovoltaics, light-emitting, and lasing devices. Bulk cut.
  - Structural and electronic features of small hybrid organic–inorganic halide perovskite clusters

- 3D bulk analysis
  - The role of the organic cation:
    - Ambipolar nature of the OIHPs.
    - Alternative, bulky, and less polarizable organic cation (FAPI/GAPI).
    - Aliovalent substitution of Pb metallic cation.
  - Slow hot-hole cooling in lead-iodide perovskite: carrier lifetime from electron–phonon interaction.
  - The effects of the organic–inorganic interactions on the thermal transport properties of MAPI.

- 0D clusters:
  - Cluster applicability in photovoltaics, light-emitting, and lasing devices. Bulk cut.
  - Structural and electronic features of small hybrid organic–inorganic halide perovskite clusters

- 3D bulk analysis
  - The role of the organic cation:
    - Ambipolar nature of the OIHPs.
    - Alternative, bulky, and less polarizable organic cation (FAPI/GAPI).
    - Aliovalent substitution of Pb metallic cation.
  - Slow hot-hole cooling in lead-iodide perovskite: carrier lifetime from electron–phonon interaction.
  - The effects of the organic–inorganic interactions on the thermal transport properties of MAPI.

- 0D clusters:
  - Cluster applicability in photovoltaics, light-emitting, and lasing devices. Bulk cut.
  - Structural and electronic features of small hybrid organic–inorganic halide perovskite clusters

- 3D bulk analysis
  - The role of the organic cation:
    - Ambipolar nature of the OIHPs.
    - Alternative, bulky, and less polarizable organic cation (FAPI/GAPI).
    - Aliovalent substitution of Pb metallic cation.
  - Slow hot-hole cooling in lead-iodide perovskite: carrier lifetime from electron–phonon interaction.
  - The effects of the organic–inorganic interactions on the thermal transport properties of MAPI.

- 0D clusters:
  - Cluster applicability in photovoltaics, light-emitting, and lasing devices. Bulk cut.
  - Structural and electronic features of small hybrid organic–inorganic halide perovskite clusters

- 3D bulk analysis
  - The role of the orgar
    - Ambipolar nat
    - Alternative, l
    - Aliovalent
  - Slow hot-hole
    electron–pho
  - The effects of the
    properties of MAPI.

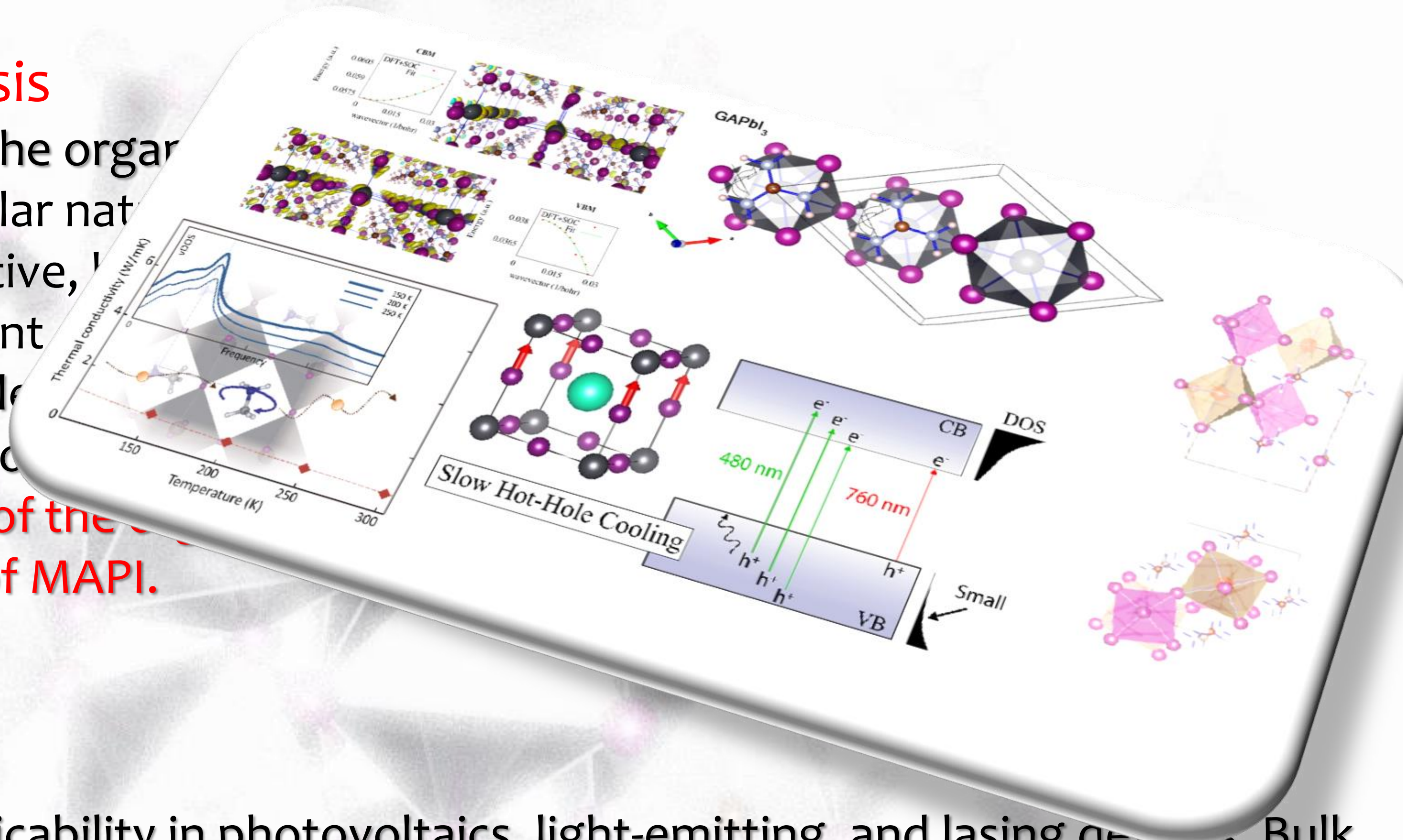

- 0D clusters:
  - Cluster applicability in photovoltaics, light-emitting, and lasing de... Bulk cut.
  - Structural and electronic features of small hybrid organic–inorganic halide perovskite clusters

- 3D bulk analysis
  - The role of the organic cation:
    - Ambipolar nature of the OIHPs.
    - Alternative, bulky, and less polarizable organic cation (FAPI/GAPI).
    - Aliovalent substitution of Pb metallic cation.
  - Slow hot-hole cooling in lead-iodide perovskite: carrier lifetime from electron–phonon interaction.
  - The effects of the organic–inorganic interactions on the thermal transport properties of MAPI.

- 0D clusters:
  - Cluster applicability in photovoltaics, light-emitting, and lasing devices. Bulk cut.
  - Structural and electronic features of small hybrid organic–inorganic halide perovskite clusters

- 3D bulk analysis
  - The role of the organic cation:
    - Ambipolar nature of the OIHPs.
    - Alternative, bulky, and less polarizable organic cation (FAPI/GAPI).
    - Aliovalent substitution of Pb metallic cation.
  - Slow hot-hole cooling in lead-iodide perovskite: carrier lifetime from electron–phonon interaction.
  - The effects of the organic–inorganic interactions on the thermal transport properties of MAPI.

- 0D clusters:
  - Cluster applicability in photovoltaics Bulk cut.
  - Structural and electronic features ide perovskite clusters

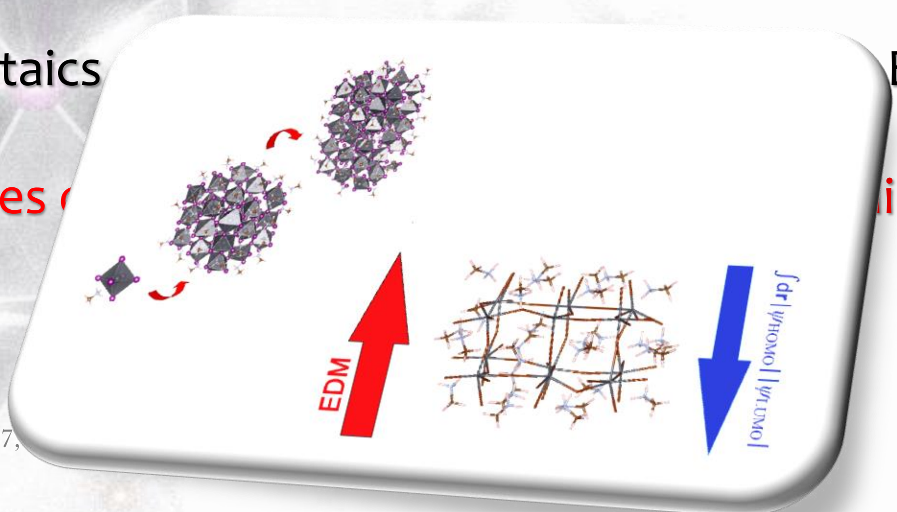

- **Ambipolar nature of the OIHPs. (the case of $MAPbI_3$, MAPI)**

Bandstructure of the bare fully optimized $[PbI_3]^-$ network (no MA)

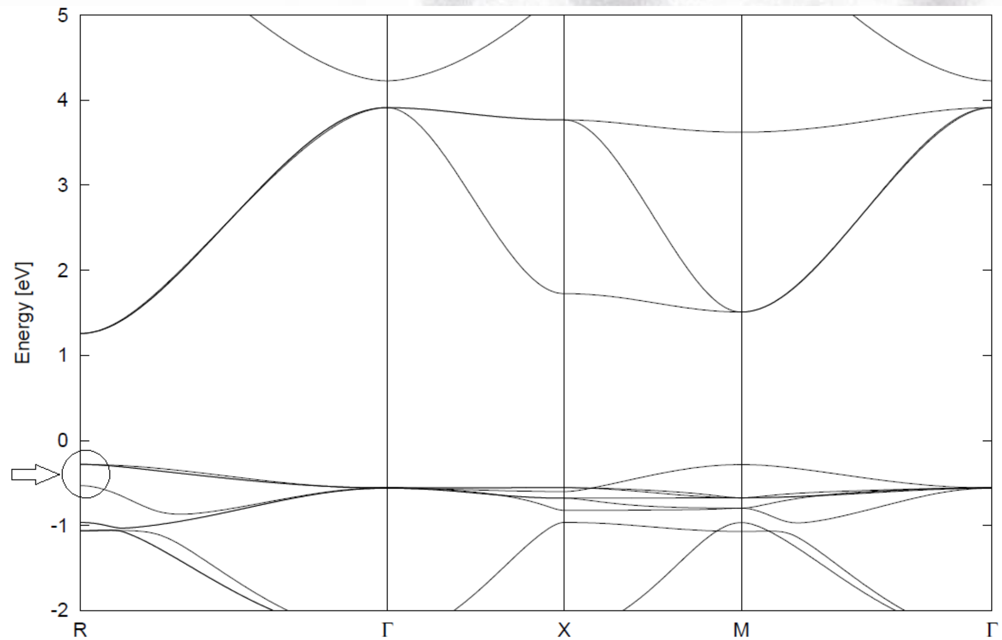

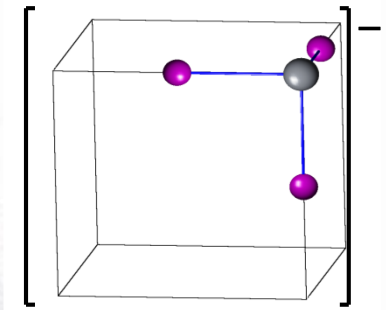

Macroscopic effects associated to cation removal:

1) Cubic symmetry recovered.

2) Expansion of the cell volume:

-Ideal crystal shows a very sensitive change (*flattening*) of the VBM shape.

VBM : 5*p* orbitals of I atoms.

Now the Pb 6s ones (mixed with I 5p orbitals) are 0.25 eV below the new VBM.

$MAPbI_3$ (DFT+SOC)

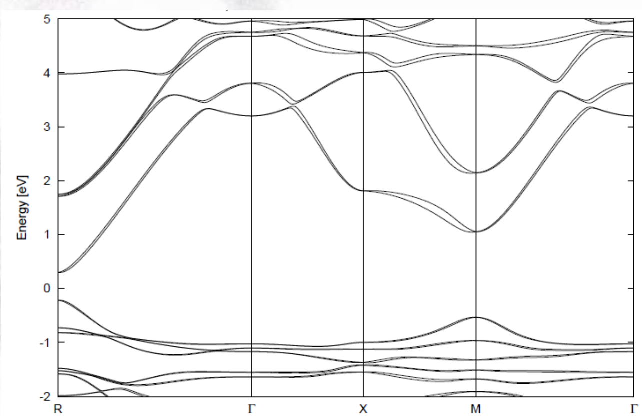

-No methylammonium (MA), no ambipolarity

- **Alternative, bulky, and less polarizable organic cation (FAPI/GAPI).**

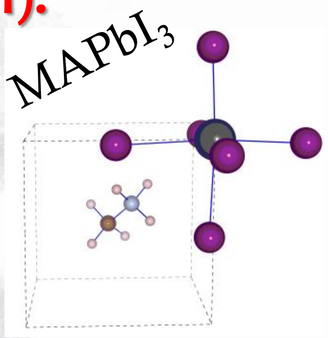

- ***Pros***:

- high compatibility with solution-based processing/good efficiencies (high absorption coefficient);
- value for the bandgap approaching the optimal value for single-junction solar cells;
- ambipolar nature of the carriers plus their very long diffusion lengths;

Cons:

-Regardless the assembling architecture, a noticeable ***hysteresis*** in the *J-V* curves is always detected. *J. Phys. Chem. Lett.*, 2014, 5 (9), pp 1511–1515

Hysteresis: slow dynamic reorganization processes & depends on several parameters:

1) scan rate of the measurements 2) the architecture of the cell

3) the perovskite deposition rate.

No conclusive explanation of its origin provided so far.

Several experimental findings ascribe it to:

1) ionic migration at an applied bias 2) ferroelectricity (?)

3) dielectric polarization in the perovskite layer.

Consistently, a *dipole-moment-reduced* cation such as formamidinium (FA) ion is reported to quantitatively reduce the hysteresis from PSCs.

G. G., K. Yamashita, *Nanotechnology*, 26 (2015) 442001.

G.G. et al., *J. Phys Chem C*, 119 (2015) 469

The organic cation role

- Kieslich et al., Chem. Sci., 2014, 5, 4712

Perovskite "classic" tolerance factor (Goldschmidt) extended to OIHP based on classical concept of ionic tolerance factors: prediction of several yet undiscovered hybrid perovskite phases.

$\alpha=(r_A+r_X)/\sqrt{2}(r_B+r_X)$

$$\boxed{\alpha=(r_{Aeff}+r_{Xeff})/\sqrt{2}(r_B+0.5h_{Xeff})}$$

$$r_{Aeff}=r_{mass}+r_{ion}$$

The organic cation role

According to the symmetry of the cation → $\mu_{GA} < \mu_{FA} << \mu_{MA}$

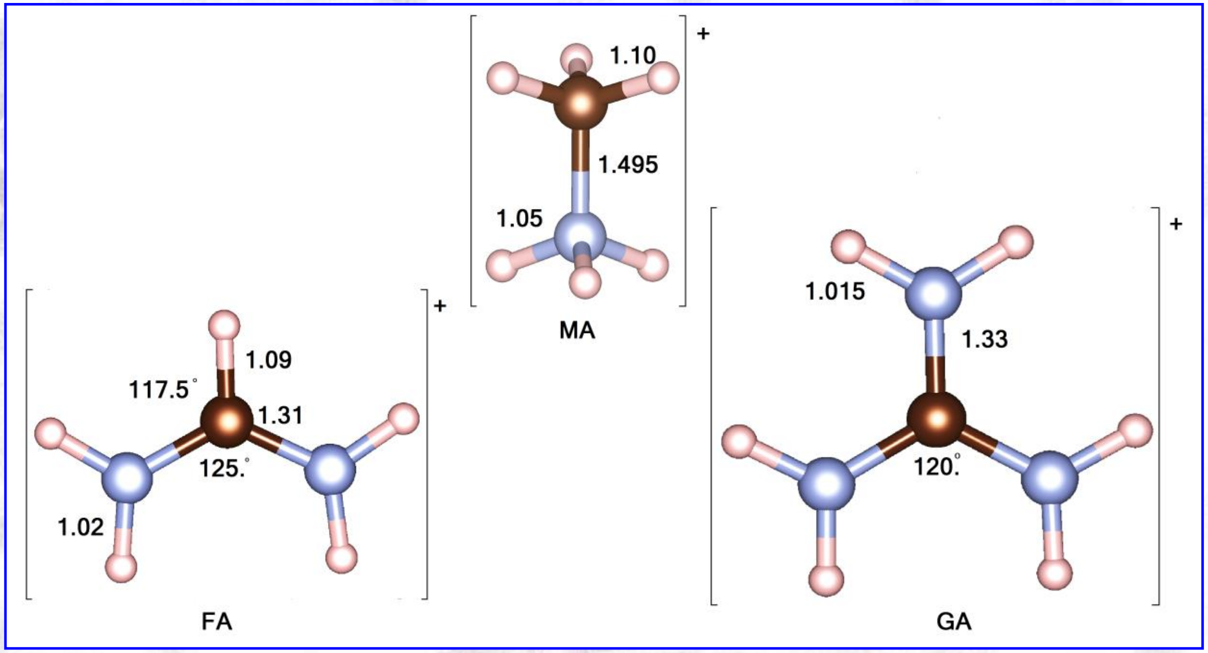

While both $MAPbI_3$ and $FAPbI_3$ (the latter characterized by trigonal P_{3m1} sym) are well known and investigated species, very few is known, and mostly at experimental level, about 3D $GAPbI_3$

G. G., K. Yamashita, *Nanotechnology*, 26 (2015) 442001.
G.G., K. Yamashita et al., *J. Phys Chem C*, 119 (2015) 469

- VASP code
- Spin-polarized DFT (PBE) & its revised version for solids (PBESol)

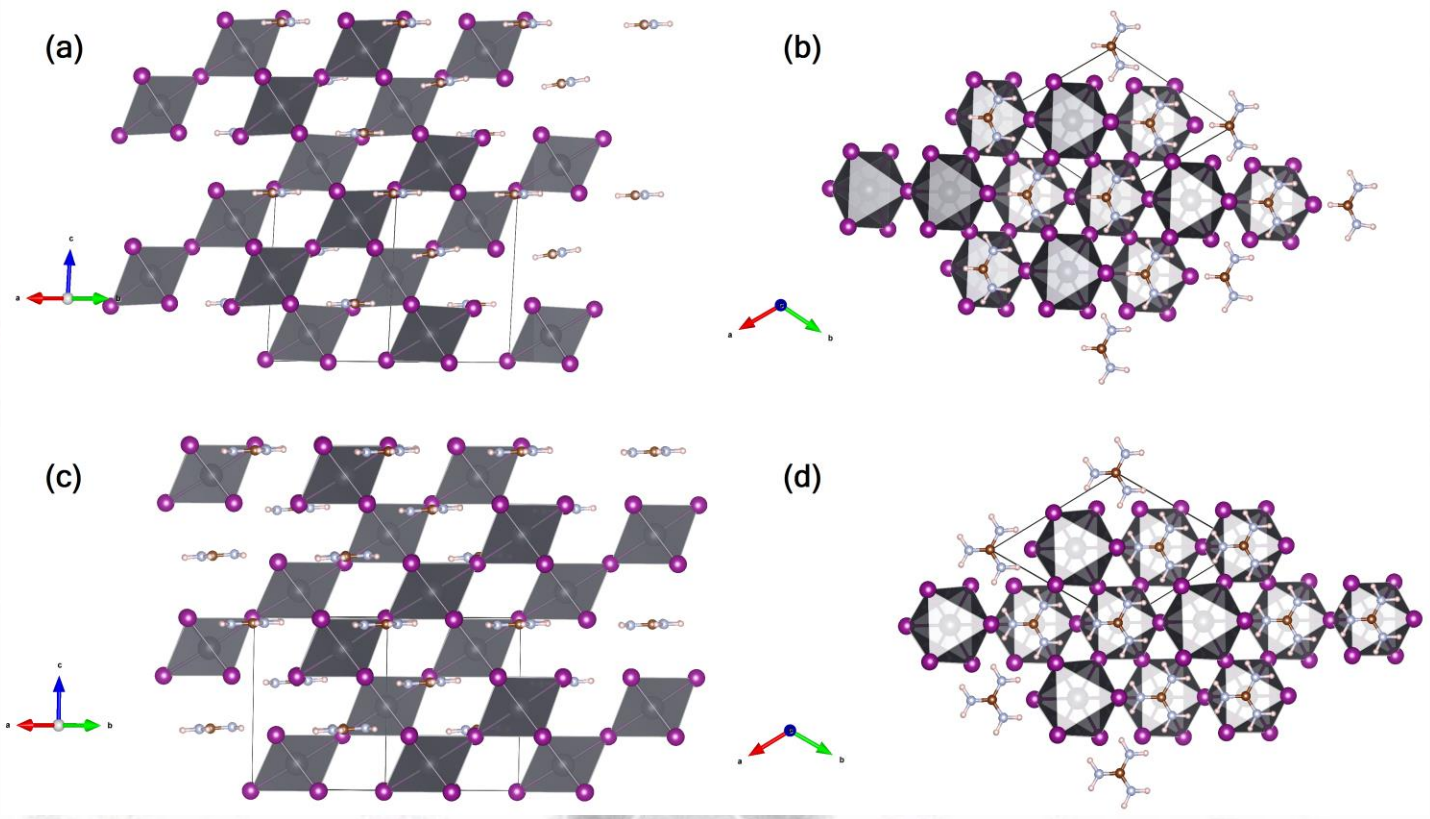

Top panel: lateral view (a) and top view (b) of the 2×2×2 optimized supercell of $FAPbI_3$.

Bottom panel: lateral view (c) and top view (d) of the 2×2×2 optimized supercell of $GAPbI_3$.

G. G., K. Yamashita, *Nanotechnology*, 26 (2015) 442001.
G.G., K. Yamashita et al., *J. Phys Chem C*, 119 (2015) 469

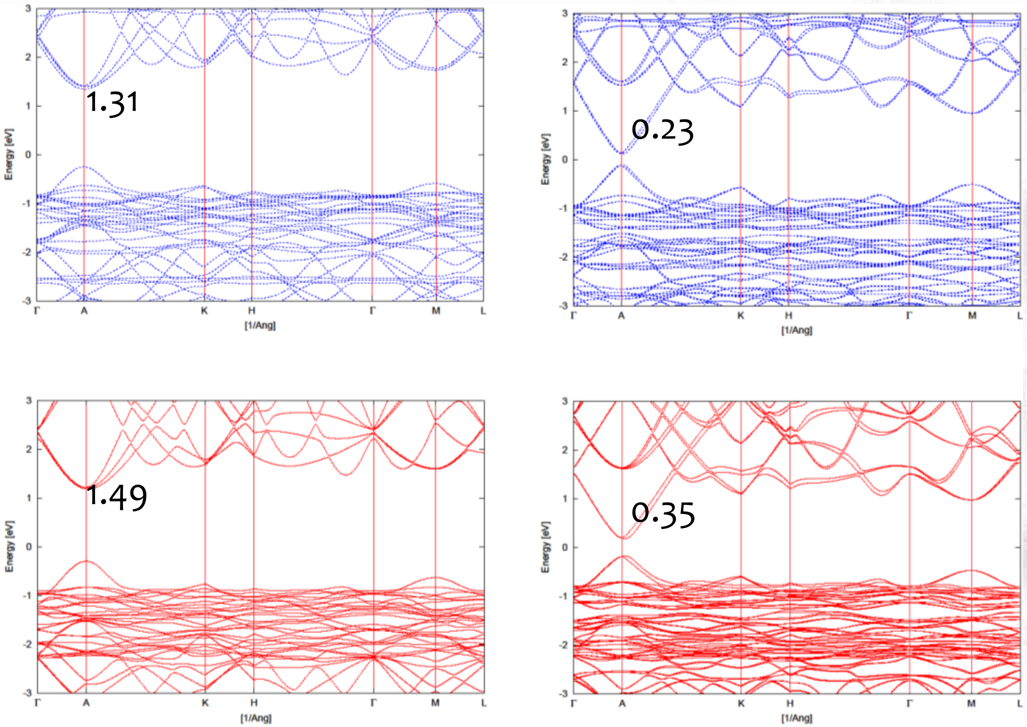

Band structure of $FAPbI_3$, calculated at PBESol/PAW (left) & PBESol/PAW+SOC (right).

Band structure of $GAPbI_3$, calculated at PBESol/PAW (left) and PBESol/PAW+SOC (right).

- Along the A–Γ direction we calculate
  - $m_h^* / m_e^* = 0.75$ $FAPbI_3$
  - $m_h^* / m_e^* = 1.07$ $GAPbI_3$

- $GAPbI_3$ has a more marked *ambipolar* behavior than $FAPbI_3$, which, still from the comparison, seems to be preferable as hole transport material.

(consistency with experimental results, *Energy Environ. Sci. 2014, 7, 982.*)

G. G., K. Yamashita, *Nanotechnology*, 26 (2015) 442001.
G.G., K. Yamashita et al., *J. Phys Chem C*, 119 (2015) 469

Chemical potential (μ) for $FAPbI_3$ & $GAPbI_3$: PAW/PBESol calculated E_{TOT}/unit , we obtain

1) $FAPbI_3 + 1/3\ GAPbI_3 \rightarrow FA_{2/3}GA_{1/3}PbI_3 + 1/3\ FAPbI_3$ $\Delta E_1 = 0.06$ eV
2) $FA_{2/3}GA_{1/3}PbI_3 + 1/3\ GAPbI_3 \rightarrow FA_{1/3}GA_{2/3}PbI_3 + 1/3\ FAPbI_3$ $\Delta E_2 = -0.03$ eV
3) $FA_{1/3}GA_{2/3}PbI_3 + 1/3\ GAPbI_3 \rightarrow GAPbI_3 + 1/3\ FAPbI_3$ $\Delta E_3 = -0.03$ eV

Processes 2-3 become exothermic revealing the stability of the intermediate mixed alloys.

The inorganic cation role

- Filip & Giustino, J. Phys. Chem. C 2016, 120, 166

Screening process based on:

1) Thermodynamic factor (the stability of the compound) in a perovskite structure.

2) Electronic factor (band gap, Eg).

The process reduces the potential candidate from 248 to 25.

15 of 25 have not yet been proposed as semiconductors for optoelectronics.

Mg_{Pb} gap is tunable over a range of 0.8 eV.

Aliovalent alloys: Pb-free perovskites

- Sn-based organic-inorganic perovskites potential alternatives to the Pb-based.
  Lower PCEs absorption onset ~ 950 nm (optical gap, 1.3 eV), red shifted compared with the Pb-based . [F. Hao et al., *Nature Photonics* **2014**, *8*, 489.]

- Mixed Pb-Sn based perovskites: further extension of the light harvesting region (~1050-1060 nm). [S. Hayase et al. *J. Phys. Chem. Lett.* **2014**, 5, 1004]

- Sn-based perovskites easily oxide ($Sn^{2+} \rightarrow Sn^{4+}$): strong *p*-type character & metallic behavior (doped semiconducting behavior).

G. G., K. Yamashita, *Chem. Lett.*, 44 (2015), 826.

- Pb replacement: alternative class of mixed organic-inorganic perovskites, i.e. $MATl_{0.5}Bi_{0.5}I_3$ (*MTBI*), where pairs of Pb(II) atoms are replaced by Tl(I)/Bi(III) *aliovalent* units.

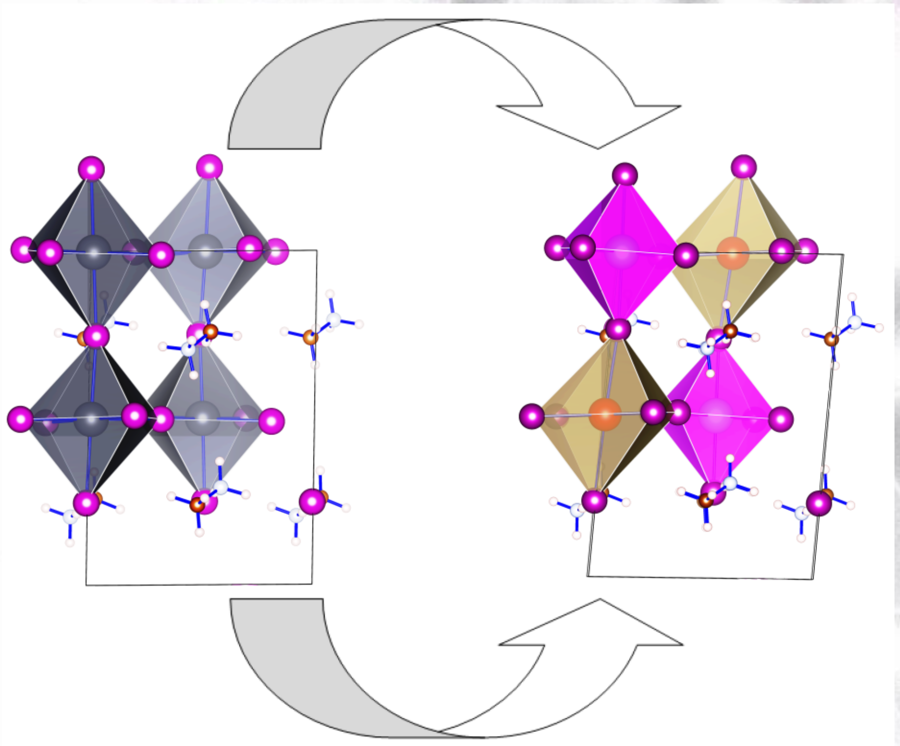

2 Pb (II) → Tl (I) + Bi (III)

- Tl similarly to Pb represents an environmental risk. Nevertheless [Tl]=0.5*[Pb]

G. G., K. Yamashita, *Chem. Lett.*, 44 (2015), 826.

Tolerance Factor calculation

- Calculation of the revised tolerance factor (α) of hybrid frameworks for "pure" $MATlI_3$, $MABiI_3$, respectively comparing the calculated value with that obtained for $MAPbI_3$ employing the formula

$$\alpha = (r_{Aeff}+r_{Xeff})/\sqrt{2}(r_B+r_{Xeff})$$

(Kieslisch et al.,*Chem. Sci.* **2014**, 5, 4712)

- I^- and MA 220 and 217 pm, Shannon ionic radius for the B-site cations

α=0.87, 0.80, and 0.92 for $MAPbI_3$, $MATlI_3$, and $MABiI_3$.

- We then considered as r_B for MTBI the averaged value (148.5 pm) of the ionic radius of Bi (117 pm) and Tl (164 pm) obtaining α=0.84.

G. G., K. Yamashita, *Chem. Lett.*, 44 (2015), 826.

Three possible structures (top view)

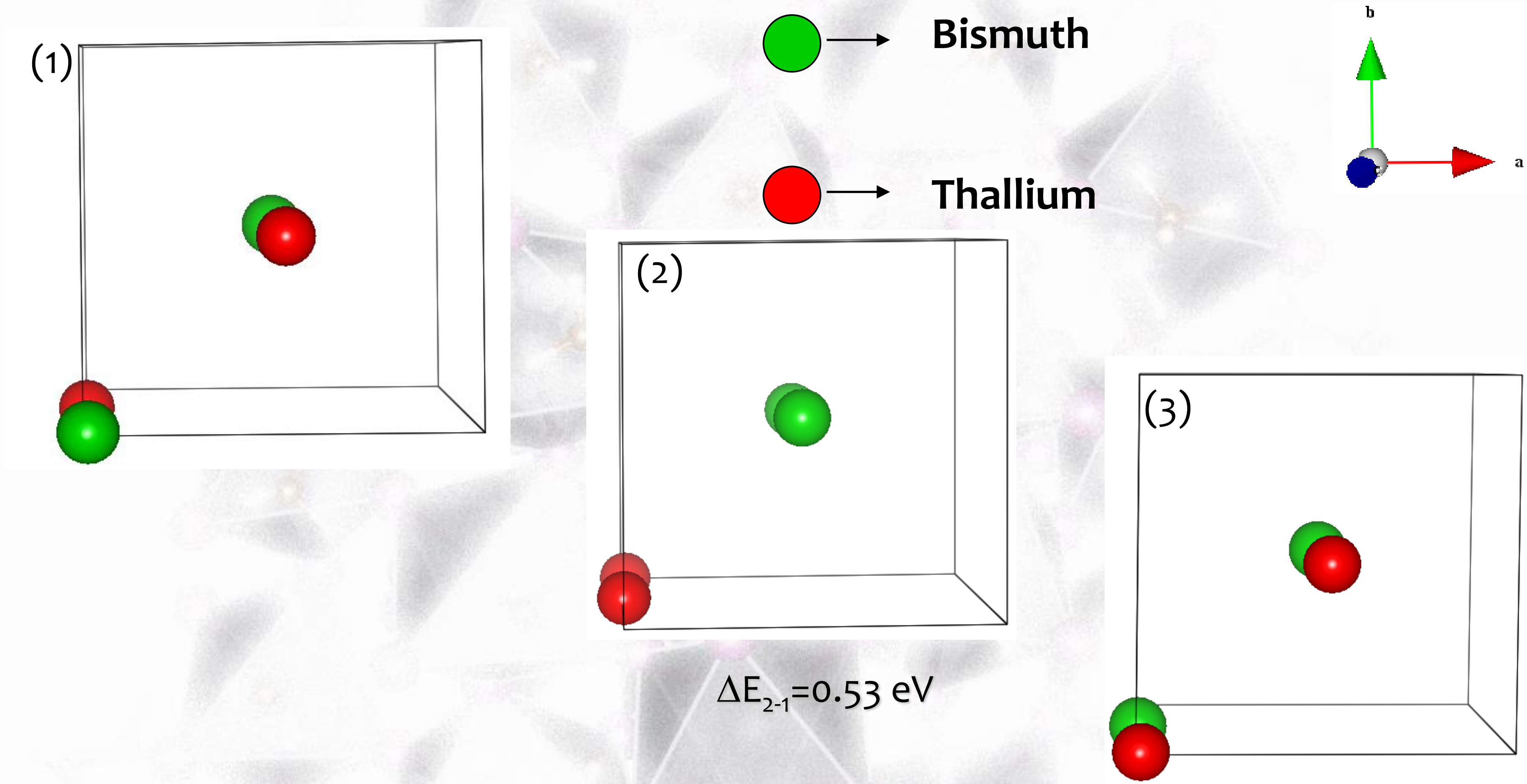

$\Delta E_{3\text{-}1}$=1.58 eV

<u>Structure (1) stabilized by a 3D self –passivating mechanism:</u>
<u>Bi & Tl as *n-/p-* centers (DFT/PAW/PBE)</u>

G. G., K. Yamashita, *Chem. Lett.*, 44 (2015), 826.

Optimized structures

Table 1. Geometrical parameters of the optimized structures of $MAPbI_3$ and MTBI (lattice parameters bondlengths, Å; Vol, Å^3; angles, degrees)

$MAPbI_3$	MTBI
$a = b = 8.92$; $c = 13.18$ $V = 1048.5$ (979.0^a, 993.8^b, 1037.4^c)	$a = 9.16$; $b = 8.91$; $c = 13.32$ $V = 1082.9$ $\alpha = 91.6$; $\beta = 85.4$; $\gamma = 89.6$
$d_{ap}(\text{Pb–I}) = 3.29, 3.32$	$d_{ap}(\text{Bi–I}) = 3.13, 3.14$ $d_{ap}(\text{Tl–I}) = 3.54, 3.55$
$d_{eq}(\text{Pb–I}) = 3.21, 3.22, 3.23,$ $3.25, 3.27, 3.29$	$d_{eq}(\text{Bi–I}) = 3.09, 3.09, 3.10, 3.14$ $d_{eq}(\text{Tl–I}) = 3.41, 3.43, 3.47, 3.48$

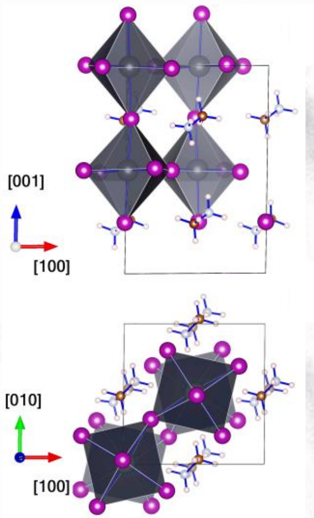

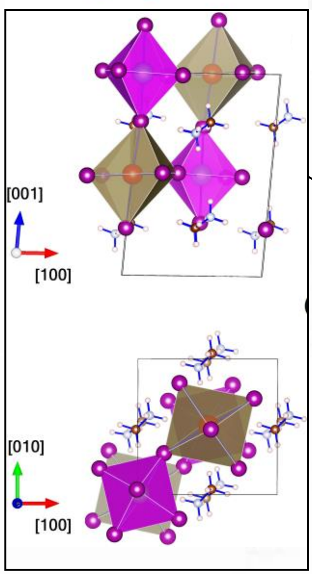

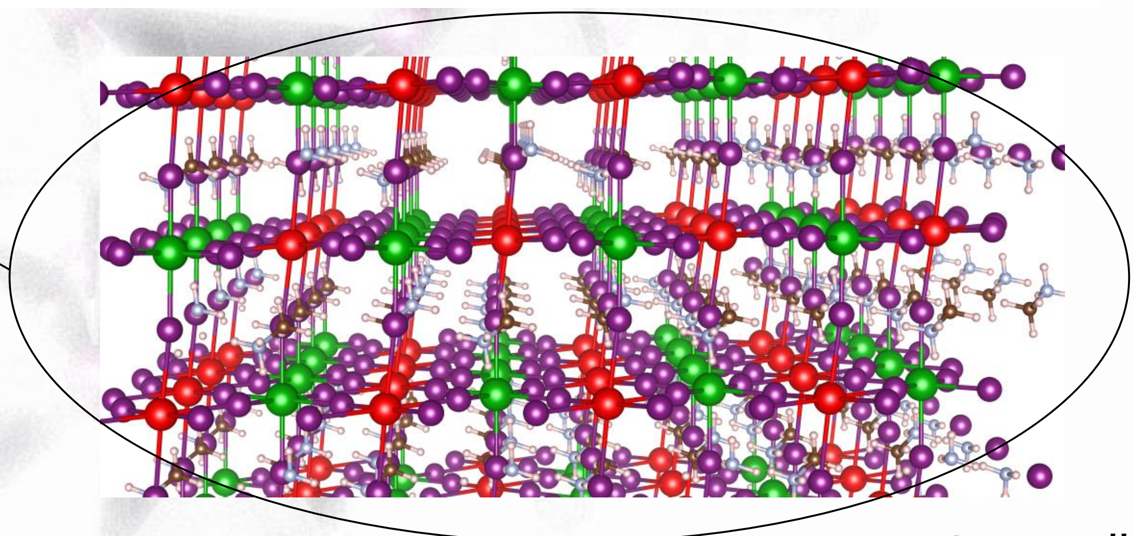

4x4 MTBI Supercell

The bandgap is direct on Γ point and it is 1.62 eV (0.74 eV) @ PBE/PAW (PBE/PAW/SOC)
μ=0.31 (0.20)
m^*_e/m^*_h =0.83

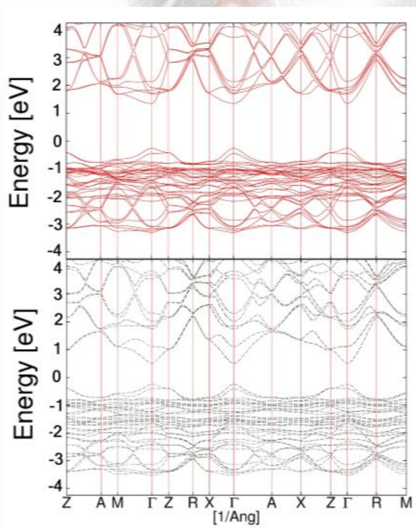

$MAPbI_3$

Reduced effective mass

$\mu = (m^*_e * m^*_h) / (m^*_e + m^*_h)$

MTBI

Bi 6*p*

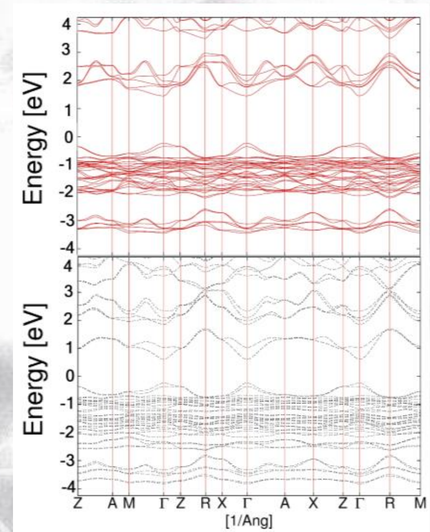

The bandgap is direct on Γ point and it is 1.68 eV (0.84 eV) @ PBE/PAW (PBE/PAW/SOC)
μ=0.33
m^*_e/m^*_h =0.89

The Mechanism of Slow Hot-Hole Cooling in Lead-Iodide Perovskite: First-Principles Calculation on Carrier Lifetime from Electron–Phonon Interaction

TAS analysis [Science 2013, 342, 344–7] : slow hot-hole cooling in $MAPbI_3$
UV–vis absorbance spectrum→ 2 main absorption peaks:

Peak @ 760 nm: direct VBM →CBM excitation.
Peak @ 480 nm? (lifetime ~0.4 ps, slow hot-hole cooling in the VB?).
Long-lived hot carriers: important for further improvements in PCE

Xing *et al*.: the two states (480 & 760 nm) composed of different VB states but same CB state.
Peak @ 480 nm: transition VB2 to CBM. (VB2=VBM-1eV)

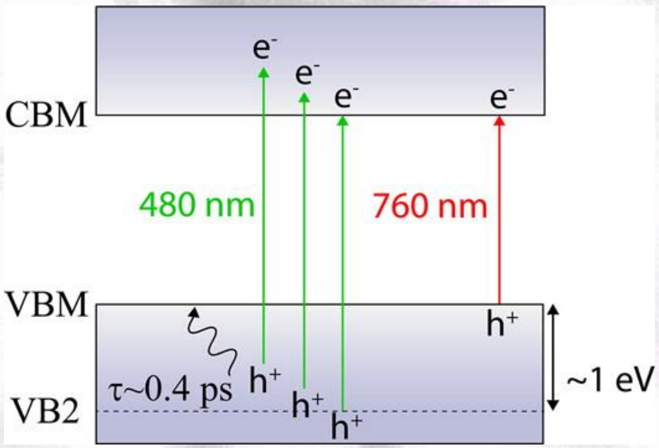

Even *et al.* proposed the optical absorption at 480 nm is composed of multibandgap absorption not only VB2 → CBM. *Is it slow hot-hole cooling observed*?

- Electron-phonon interactions by combining density-functional theory (DFT), density-functional perturbation theory (DFPT), and many-body perturbation theory (MBPT).
- Here we investigate (a) $MAPbI_3$, (b) $CsPbI_3$, and (c) PbI_3^-

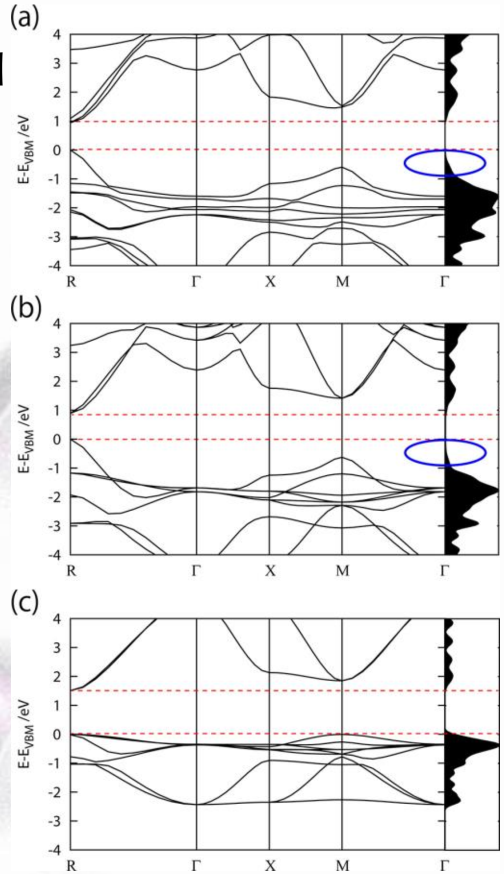

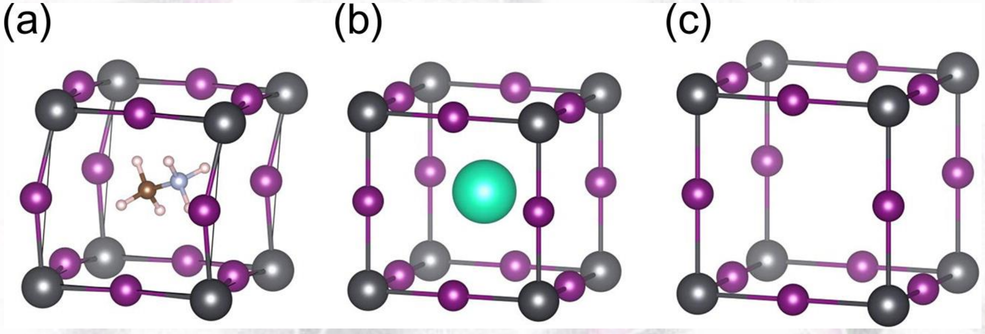

Phonons & e-ph coupling matrix: DFPT scheme by PHonon code in the PWscf.

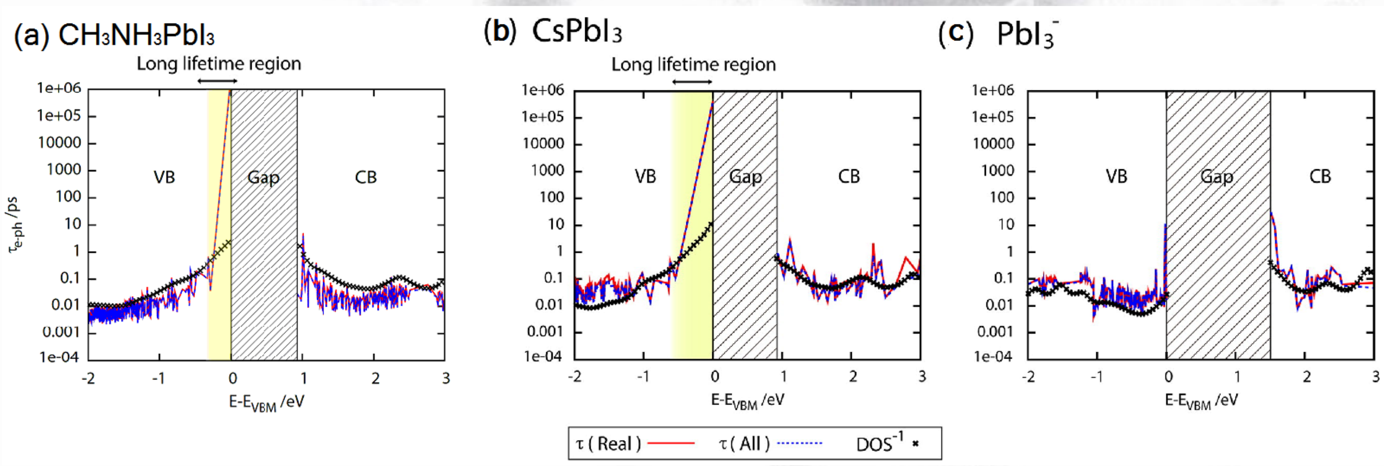

(Blue dotted lines) lifetimes with & (red solid lines) lifetimes w/o the imaginary modes. Black crosses: inverse of the DOSs

H. Kawai, G. G., A. Marini, K. Yamashita *Nano Lett*., 2015, 15,3103–3108

- Carrier decay paths: generalized Eliashberg functions of the Fan contribution [first term (H_1) of the Taylor expansion of the Hamiltonian (H_0)]
- This function defines the contribution of phonons to the carrier relaxation for each electronic state.

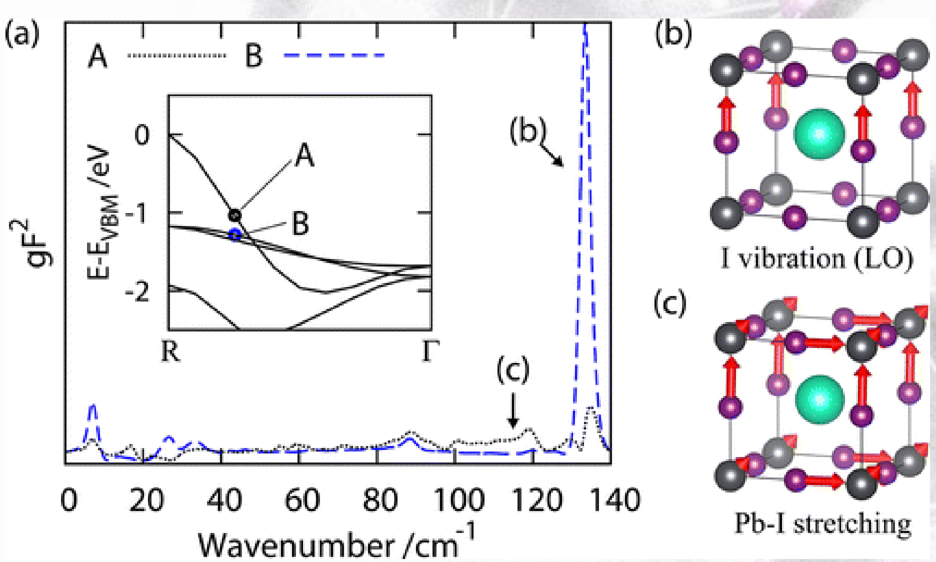

→Vibrational modes coupled with the VBs of $CsPbI_3$ are ascribed to the motions of I & Pb, ***not*** of Cs.

→The replacement of the perovskite A-site cation has no impact on the mechanism of carrier relaxation.

→ we predict that the slow hot-hole cooling is **universally** observed in $APbI_3$.

H. Kawai, G. G., A. Marini, K. Yamashita *Nano Lett.*, 2015, 15,3103–3108

From 3D to 0D: Perovskite Nanoclusters

Three- and low-dimensional inorganic semiconductors

G.C. Papavassiliou

(Prog. Solid State Chem. 1997, 25, 125-270)

- 0D $(CH_3NH_3)_3Bi_2I_9$ perovskite for optoelectronic applications

(Öz et al. Solar Energy Materials and Solar Cells, 2016)

Solar cells assembled with 0D bismuth based perovskites, with enhanced stability, towards moisture, with respect to 3D lead and tin-based ones. ☺ ☺ ☺

- Pure Cs_4PbBr_6 and its extremely high luminescence.PLQY (PL Quantum Yield) ~ 40% (high exciton BE~353 meV)

Color-converting and light emitting applications

(Saidaminov et al. , ACS Energy Lett., 2016 1, 840).

(Protesescu et al., Nano Lett., 2015, 15, 3692.)

Design of highly luminescent perovskite-based colloidal quantum dot materials.

Colloidal nanocubes of CsPbX3 (X = halide)

Composition and quantum size-effects:

E_{gap} & emission spectra tunable over the VIS region .

PL of $CsPbX_3$ nanocrystals:

narrow emission (very good for blue and green spectral regions)

From 3D to 0D: MAPbI3 Nanoclusters

Modellization motivated by the lack of experimental and theoretical results about OIHP nanostructures in view of their fundamental property investigations.

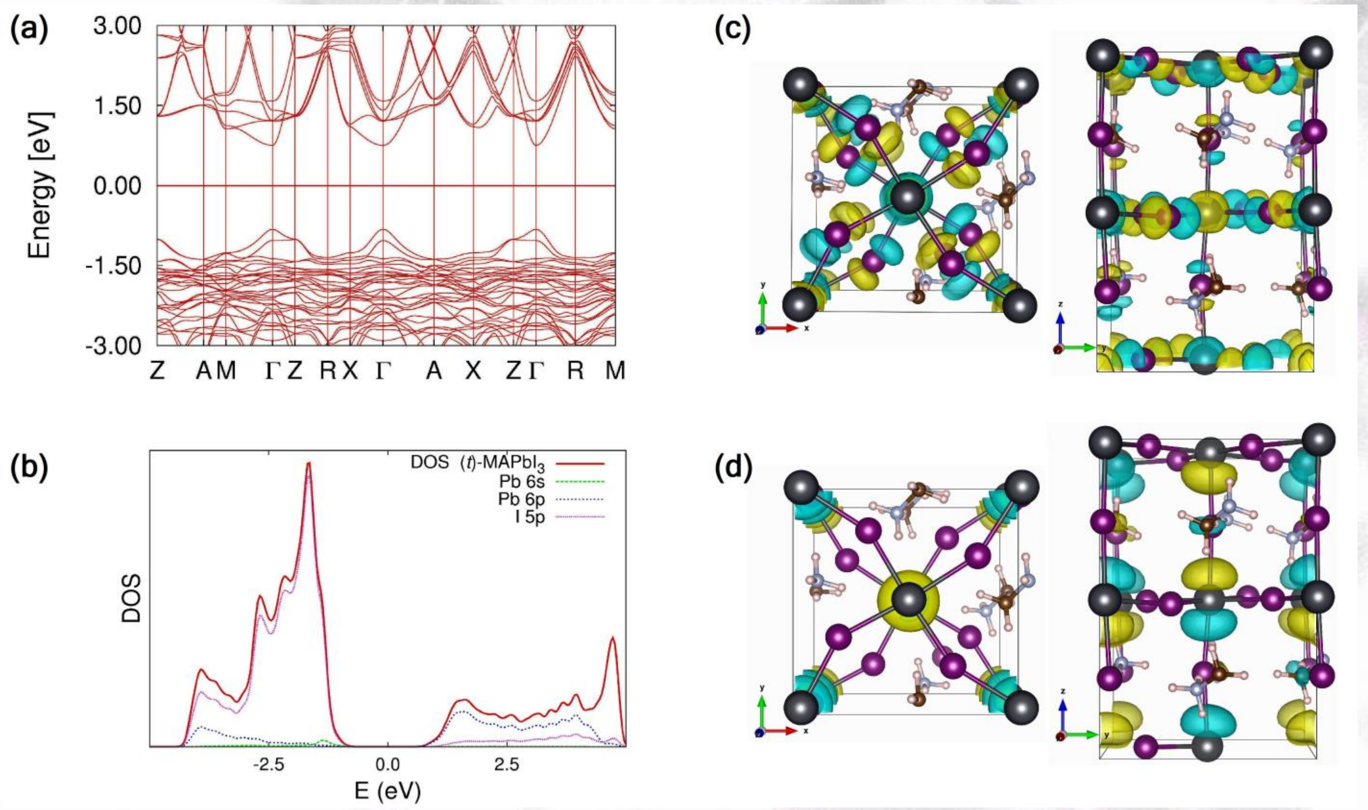

Localized Atomic Orbitals (SIESTA)

(a) PAO/PBE calculated bandstructure and (b) PDOS for *t*-$MAPbI_3$. (c) lateral and top view of VBM, and (d) lateral and top view of the CBM of *t*-$MAPbI_3$

G. G., K. Yamashita, *J. Phys. Chem. Lett.*, 7 (2016) 888. Perspective article.

3 Nanocluster models

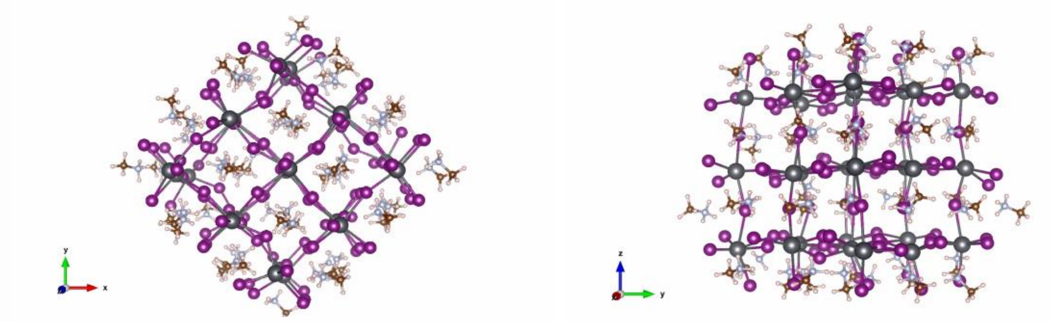

-$MA_{54}Pb_{27}I_{108}$, (567 atoms, ***1s***): regular 3x3x3 grid of 6-fold Pb atoms with 54 MA groups with an organic/inorganic cation ratio of 2.00. Fully MAI-terminated.

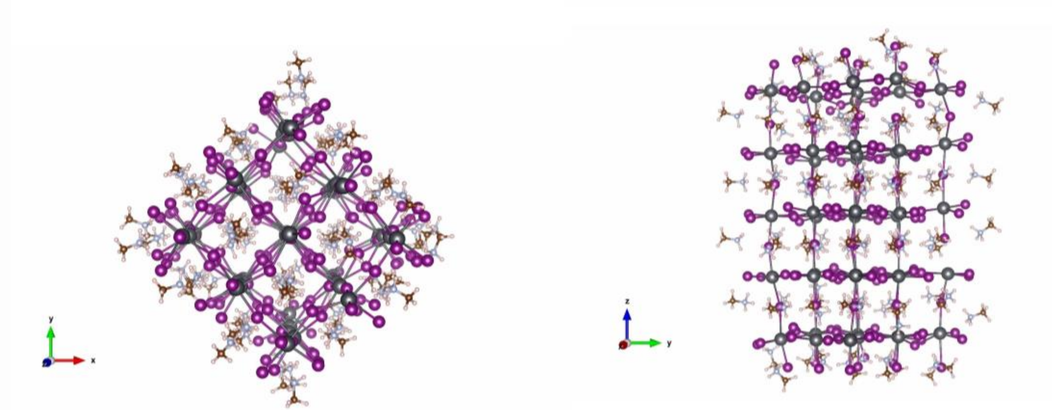

-$MA_{84}Pb_{45}I_{174}$: 3x3x5 fully MAI-terminated with an organic/inorganic cation ratio of 1.87 (891 atoms, 60 dangling I atoms, ***2i***).

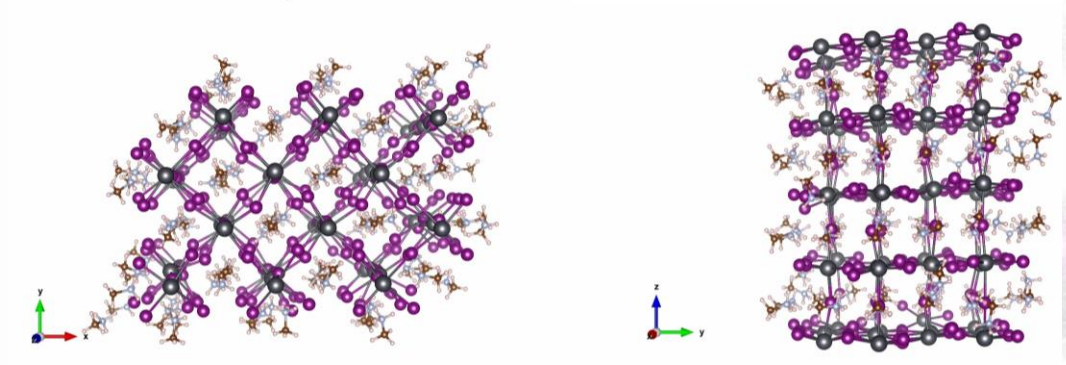

-$MA_{93}Pb_{60}I_{213}$ with a final organic/inorganic cation ratio of 1.55. (1017 atoms, ***3l***)
PbI2 (MAI)-terminated along z (*xy*)

G. G., K. Yamashita, *J. Phys. Chem. Lett.*, 7 (2016) 888. Perspective article.

Pb27 & Pb60 (NVE, 3ps, t=0.25fs)

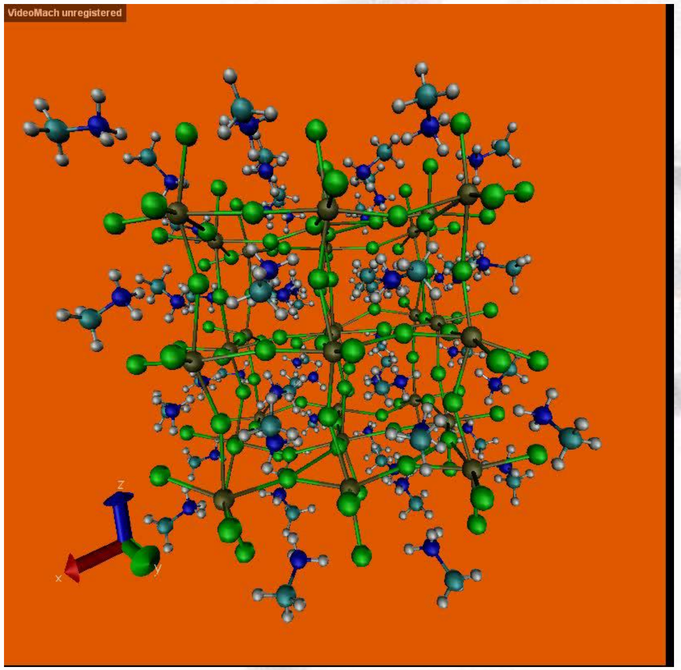

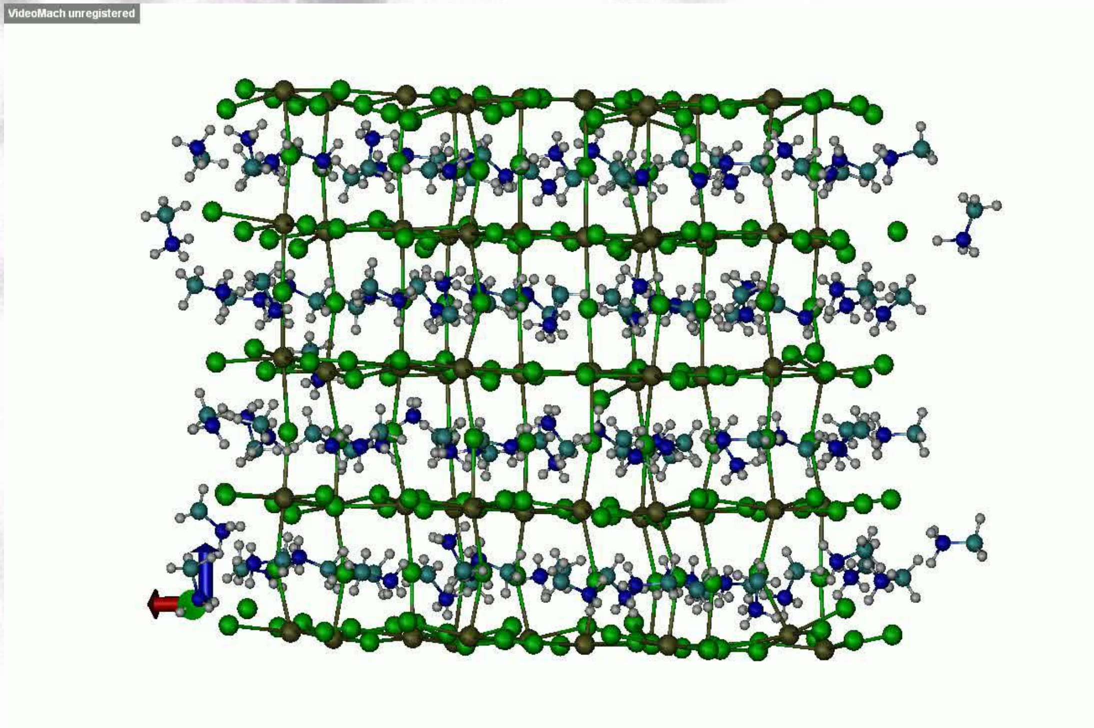

Electronic Properties (DOS)

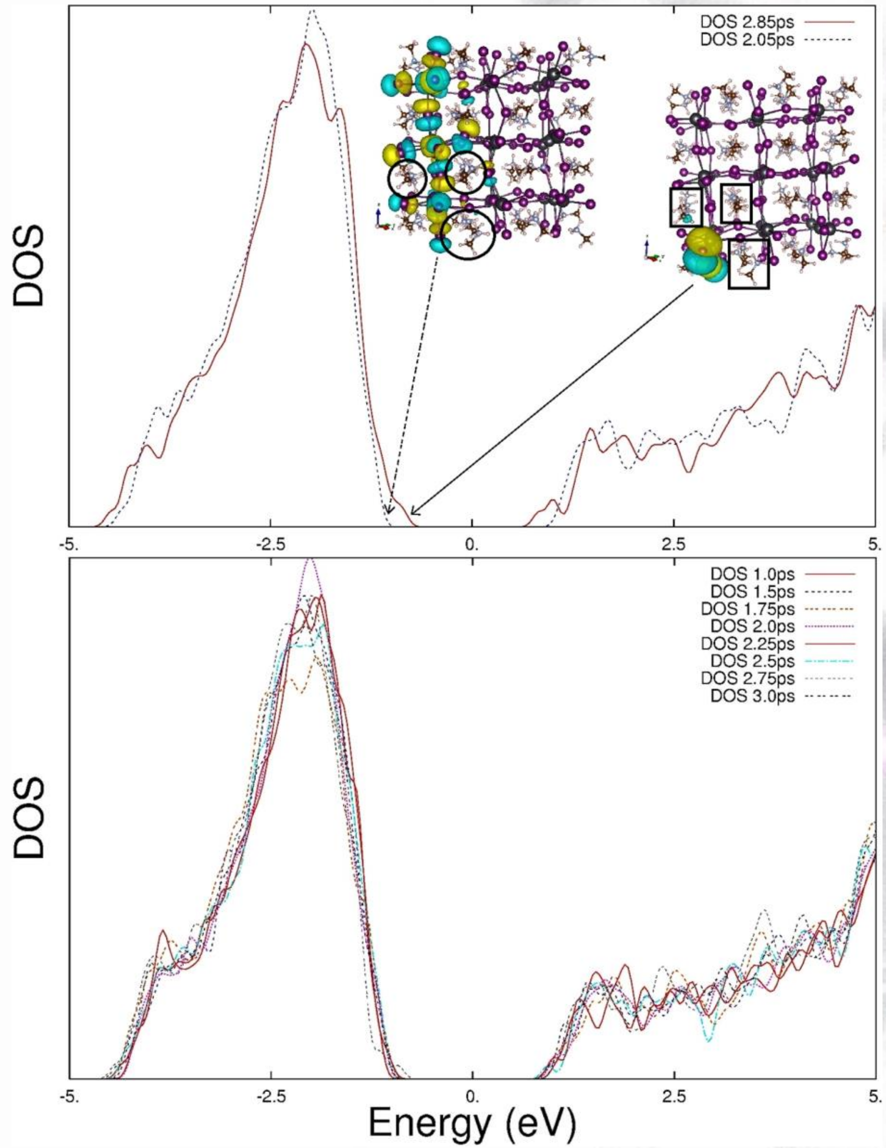

- DOS of the trajectory at 2.85ps (2.05ps) for the ***1s*** cluster.

- DOS evolution for the ***1s*** cluster along the whole MD run

G. G., K. Yamashita, *J. Phys. Chem. Lett.*, 7 (2016) 888. Perspective article.

Angular velocity of MA cation

- As a first approximation, to calculate the angular velocity, we consider the variation of the *z*-coordinate of the same C atoms between 2 selected trajectories in the AIMD simulation

$$arcsin\,(z_C^{I} - z_C^{II}) = d\phi \qquad \omega = d\phi / dt.$$

- 3 different MA cations:
  1 embedded in the network
  2 at the surface, i.e., 1 at the corner ; 1 in the middle of the (001) surface.
  3 trajectory (@~2 ps, 2.0625 ps, 2.125 ps).

  For the internal MA of ω = 0.09 deg/fs, (2.0625 ps-2 ps & 2.125 ps-2 ps).
  ω = 0.10 deg/fs (2.125 ps -2.0625 ps) .
- For the external MA cations.
  ω (MA @001 surface) = 0.26 deg/fs, 0.28 deg/fs, 0.28 deg/fs
  ω (MA @ the corner) = 0.11 deg/fs, 0.22 deg/fs, 0.33 deg/fs.

G. G., K. Yamashita, *J. Phys. Chem. Lett.*, 7 (2016) 888. Perspective article.

Structural & electronic features of small hybrid OIHP clusters

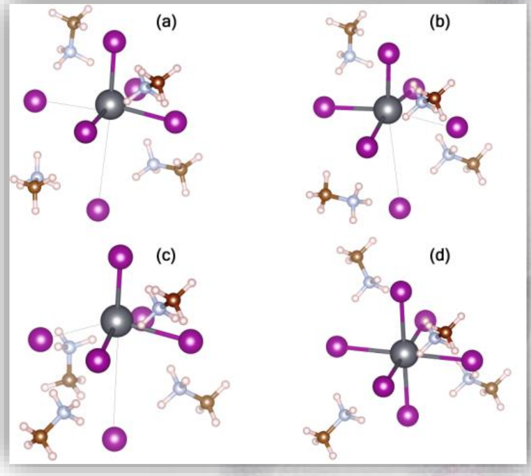

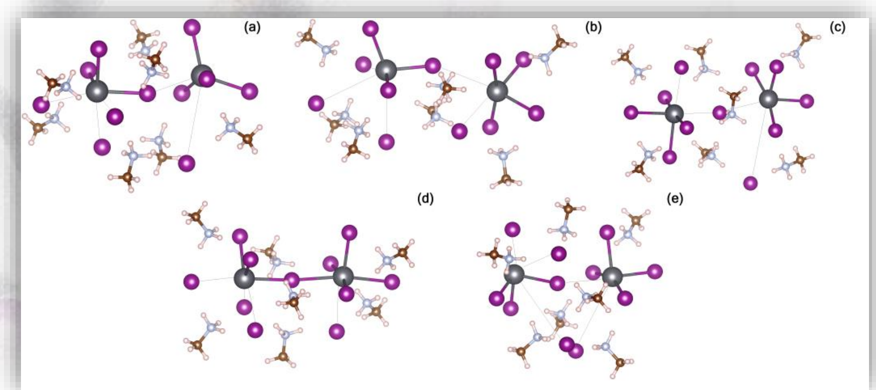

$(MA)_jPb_kX_l$ (l= 2j+k; MA=$^+CH_3NH_3$; X=halide) (k=1, 2, 8, 12) Gaussian09 code

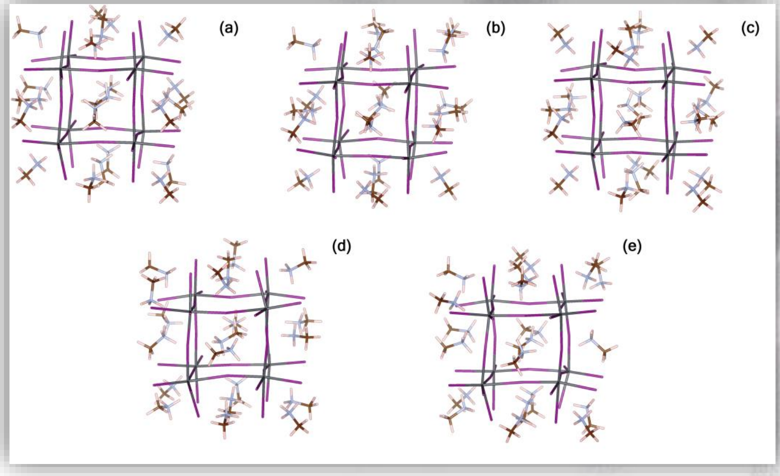

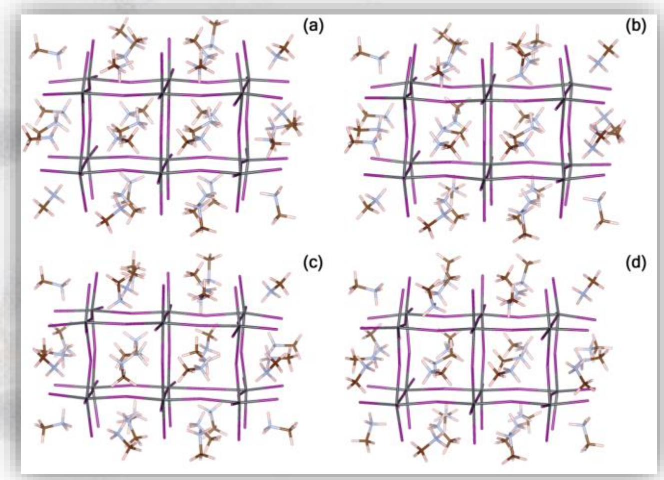

G. G., T. Yoshihara, K. Yamashita, *Phys. Chem. Chem. Phys.* (2016) 18, 27124.

Single octahedron (k=1) @ DFT

Model	Energy	E_g	ε_r
1a	+0.3844	4.410	
1b	+0.2274	4.248	
1c	+0.0069	4.468	
1d	—	4.674	2.723
		(3.947)	
1d (MA_4PbI_5Br)		4.703	2.664
1d ($MA_4PbI_4Br_2$)		4.758	2.608
1d ($MA_4PbI_3Br_3$)		4.892	2.546
1d ($MA_4PbI_2Br_4$)		4.966	2.503
1d (MA_4PbIBr_5)		5.055	2.474
1d (MA_4PbBr_6)		5.263	2.426

- As for the bulk, the gap redshift depends on the reduced electronegativity of the halide that enhances the degree of covalency of the Pb-X bond.

- MHF78 instead of MWB78 for Pb

In the nonlinear variation of E_g as function of the composition:

$$E_g[MA_4\,Pb(I_{1\text{-}x}Br_x)_6] = \\ = E_g[MA_4PbI_6] - (E_g[MA_4PbBr_6]\text{-}b)x + bx^2$$

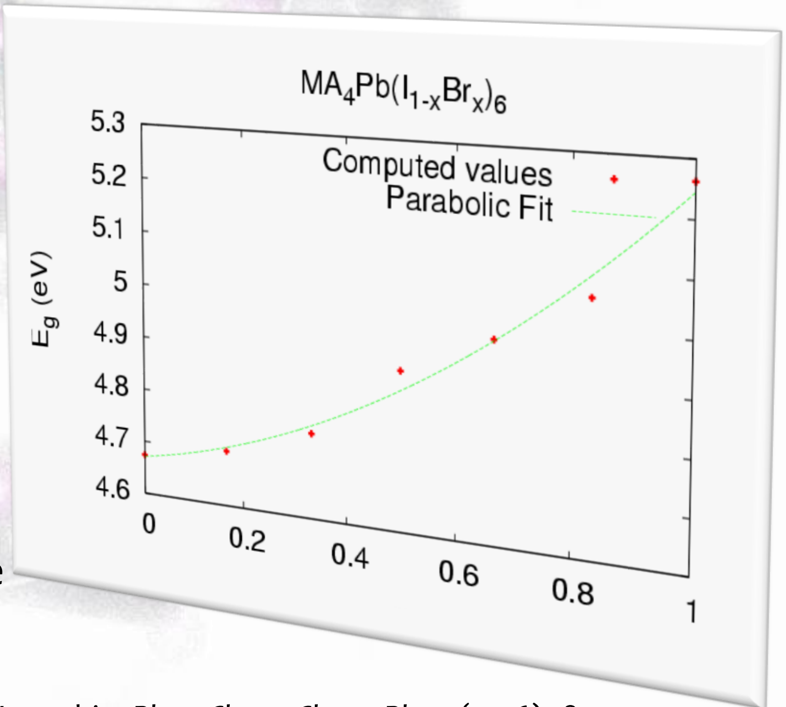

The parabolic fit that changes the eq. into:

$$\boxed{E_g(x) = 4.67 + 0.17x + 0.40x^2}$$

b=0.40, close to the experimental value (0.33 eV) for the bulk case (miscibility originates at the cluster level).

G. G., T. Yoshihara, K. Yamashita *Phys. Chem. Chem. Phys.* (2016) 18, 27124.

Octamer & dodecamer (k=8, 12)

- Relationship between TOTAL electric dipole moment (EDM) *vs* FMO wavefunction localization

- EDM described by defining the «center» of the orbital as:

$$\frac{\int d\boldsymbol{r}\boldsymbol{r}\,|\psi(\boldsymbol{r})|^2}{\int d\boldsymbol{r}|\psi(\boldsymbol{r})|^2}$$

- HOMO/LUMO separation quantified via the overlap integral:

$$S = \int d\boldsymbol{r}|\psi_{\mathrm{HOMO}}||\psi_{LUMO}|$$

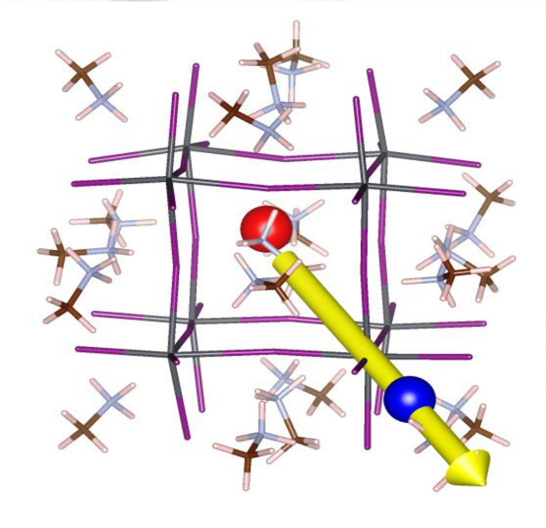

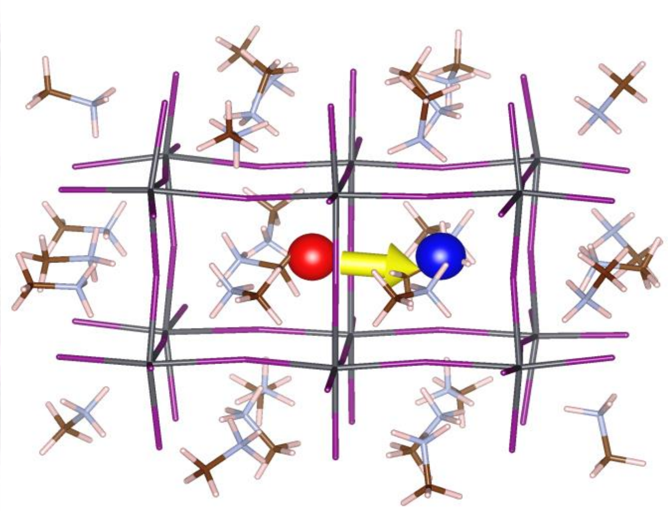

G. G., T. Yoshihara, K. Yamashita, *Phys. Chem. Chem. Phys.* (2016) 18, 27124.

Octamer & dodecamer (*k*=8, 12)

Relationship between the EDM and the calculated overlap integrals (*S*), in Pb octamers & dodecamers.

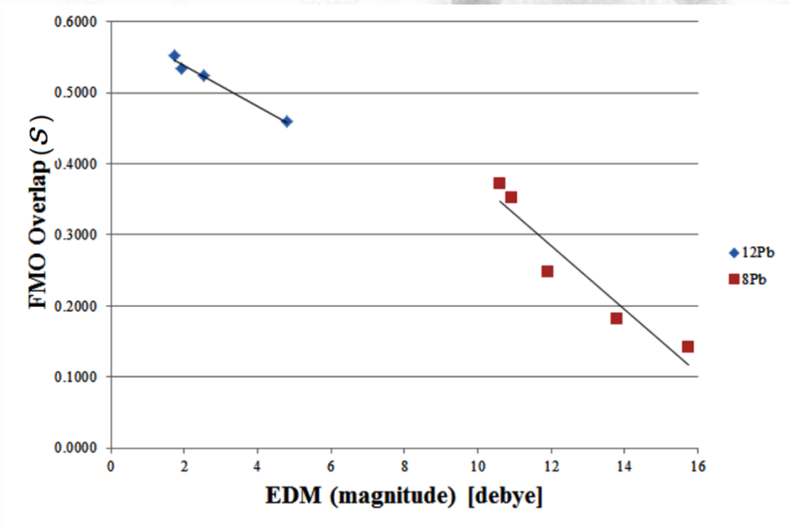

Relationship between the EDM and the calculated overlap integrals (*S*), in 12 Pb (X=Br).

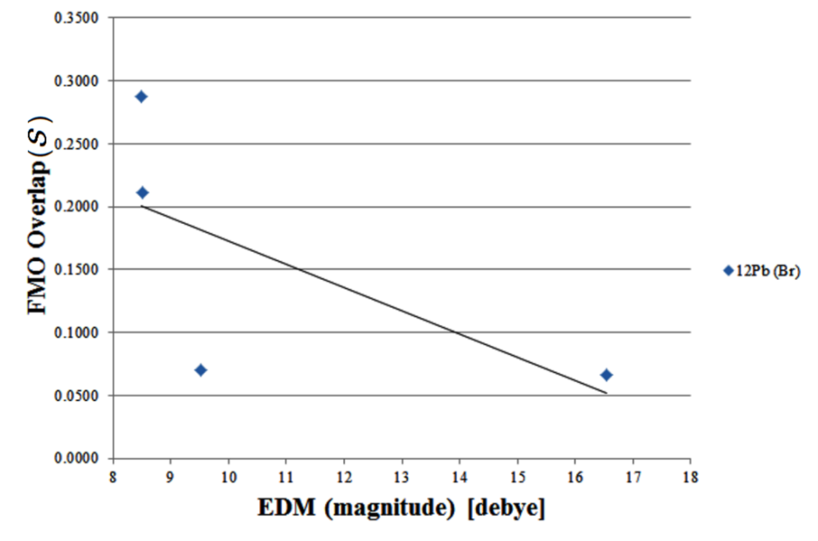

As the EDM increases the FMO overlap decreases (enhanced separation between HOMO & LUMO)

G. G., T. Yoshihara, K. Yamashita, *Phys. Chem. Chem. Phys.* (2016) 18, 27124.

Acknowledgements

- Prof. Koichi Yamashita (The University of Tokyo)

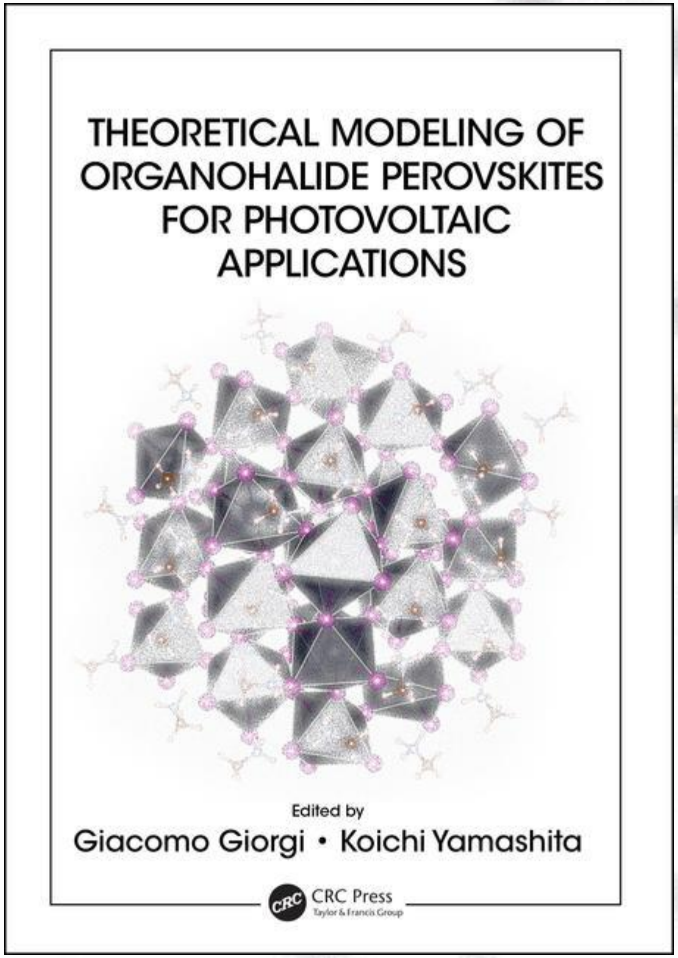

Dr. Hiroki Kawai
Dr. Tomoyuki Hata
Dr. Tomohiro Yoshihara

Some bibliography

G. G., T. Yoshihara, K. Yamashita**,**
"Structural and electronic features of small hybrid organic–inorganic halide perovskite clusters: a theoretical analysis"
Phys. Chem. Chem. Phys. (2016) 18, 27124.

G.G., K. Yamashita,
"Zero-Dimensional Hybrid Organic–Inorganic Halide Perovskite Modeling: Insights from First Principles"
J. Phys. Chem. Lett. (2016) 7, 888. (*Perspective article)*.

G.G., K. Yamashita,
"Zero-dipole molecular organic cations in mixed organic–inorganic halide perovskites: possible chemical solution for the reported anomalous hysteresis in the current–voltage curve measurements"
Nanotechnology, 26 (2015) 442001. (Invited to 'Perovskite Solar Cells' , Sum & Park Editors, themed issue paper, *Topical Review Article*)

G.G., K. Yamashita,
"Organic-Inorganic halide perovskites: an ambipolar class of materials with enhanced photovoltaic performances"
J. Mater. Chem. A 3 (2015) 8981 (Invited to 'Perovskite Solar Cells' , Lin, Park, and Li Editors, themed issue paper, *Review Article*)

G.G., K. Yamashita,
"Alternative, lead-free, hybrid organic-inorganic perovskites for solar applications: a DFT analysis",
Chem Lett. 44 (2015) 826.

G.G., J.-I. Fujisawa, H. Segawa, K. Yamashita
"Organic-Inorganic hybrid Lead-Iodide Perovskite Featuring Zero-Dipole-Moment Guanidinium Cations: A Theoretical Analysis"
J. Phys Chem C, 119 (2015) 4694. (*Editor's Choice*).

H. Kawai, **G.G.**, A. Marini, K. Yamashita
"The mechanism of slow hot-hole cooling in lead-iodide perovskite: First-principle calculations on electron-phonon carrier lifetimes"
Nano Lett., 15 (2015) 3103.

G.G., J.-I. Fujisawa, H. Segawa, K. Yamashita
"Cation Role in Structural and Electronic Properties of 3D Organic-inorganic Perovskite Halides: A DFT Analysis"
J. Phys. Chem. C, 118 (2014) 12176.

J.-I. Fujisawa, **G.G.,**
"Lead-iodide nanowire perovskite with methylviologen showing interfacial charge- transfer absorption: a DFT analysis"
Phys. Chem. Chem. Phys., 16 (2014) 17955.

G.G., J.-I. Fujisawa, H. Segawa, K. Yamashita
"Small Photocarrier Effective Masses Featuring Ambipolar Transport in Methylammonium Lead Iodide Perovskite: A Density Functional Analysis"
J. Phys. Chem. Lett., 4 (2013) 4213.